Hindawi
Advances in Civil Engineering
Volume 2019, Article ID 1795958, 20 pages
https://doi.org/10.1155/2019/1795958

Review Article

A Synthesis of Computational and Experimental Approaches of Evaluating Chemical, Physical, and Mechanistic Properties of Asphalt Binders

Kamal Hossain[1] **and Zahid Hossain**[2]

[1]*Department of Civil and Environmental Engineering, University of Illinois at Urbana-Champaign, Urbana, IL, USA*
[2]*Department of Civil and Environmental Engineering, Arkansas State University, Jonesboro, AR, USA*

Correspondence should be addressed to Kamal Hossain; kamalh@mun.ca

Received 6 February 2018; Revised 10 May 2018; Accepted 4 June 2018; Published 3 February 2019

Academic Editor: Yuqing Zhang

Asphalt binder is a very complex chemical compound. Much work has been done to understand and model its chemical, morphological, rheological, and mechanical features. This paper synthesizes and presents findings from pertinent studies available in the public domain. Understanding of asphalt characteristics at the very finite level is the first critical step to develop a better macroscopic- or pavement-level performance model. This paper showcases a summary of current knowledge gained on (a) how chemical elemental compositions and molecular groups play critical roles in asphalt binder's performance in pavement composites; (b) morphological properties and their relationships with the asphalt's structural performance; and (c) mechanistic characteristics of asphalt binder's at nanoscopic, mesoscopic, and microscopic levels, and how they are related to macroscopic- or pavement-level performance.

1. Introduction

About 96% of paved roads in the U.S. are made of asphalt [1]. Most of these roads were built during and immediately after the Second World War. They demand major rehabilitation or reconstruction services. The most expensive element in asphalt pavement is the asphalt binder. Government agencies not only in the U.S. but also around the world spend significant resources to develop a total design package that can result in a longer lasting pavement and be economic to build and maintain. In the recent decades, a common practice that many agencies adopted to reduce expenditure is recycling of existing old pavements by reducing the amount of new asphalt binder. Asphalt researchers have expressed their concerns to this strategy because the use of high-grade asphalt binder from existing asphalt pavements can have detrimental effects on the longevity of the new pavement. Valid reasons for this concern are the blending and performance issues of the aged binder, which comes from old or aged pavements.

Asphalt is also a very complex nonlinear chemical material [2]. It is complex because of its highly variable chemical constituents that change with source, process of extraction, temperature, ambient environment, and elapsed time. To better understand asphalt binder's behavior, a significant number of chemistry-based researches have been conducted in Europe and North America. In the late 1980s and early 1990s, Jennings et al. [3, 4] initiated chemical studies of asphalt binders and proposed average molecular structures for them. The ultimate goal of these research studies is to develop multiscale pavement models. The developed models should link and communicate the performance of the constituent materials among different scales (nano-, micro-, meso-, and macroscale/pavement). Pavement model features such as stiffness, rutting, and cracking performance should be found on the enhanced understanding from the finite level possible for each constituent and for all phases [5]. With the advent of new technologies, capturing of rich information of materials at micro- or nanoscale levels has become easy in the recent time, and it has successfully been utilized in other natural science and engineering disciplines. Asphalt researchers have also recently advanced knowledge related to binder

performance at much needed microscopic level, which is more important than meso- or macroscale [6–8]. Based on findings of the existing literature, it is clear that the behavior of asphalt pavement materials depends highly on their microstructure. For instance, cracks and voids at the microstructure level can eventually lead to failures of the material under loads [9]. Thus, understanding the deterioration process and improving the materials at the microstructure level can help in constructing longer lasting pavement. A better understanding of microstructure of asphalt binders is also expected to help researchers to develop better models for predicting pavement performance.

The main goal of this study is to synthesize the understanding of asphalt binder at microscopic level. To accomplish the aforementioned goal, a thorough review of pertinent literature has been conducted and presented in a coherent format. This paper is organized in multiple sections. As seen here, the current section provides an introduction to the topic. The second section presents a summary of understanding of chemical constituents and chemical models of asphalt binder. The third section discusses the morphological models and how these models correlate with chemical models. The fourth section presents the mechanistic models and their relationship with macroscopic or pavement models. Finally, the concluding section presents an overall development in the topic and gives a future research direction.

2. Chemical Models of Asphalt

A very rich amount of information is available in the literature on the chemistry of asphalt. The information includes the types and percentages of elemental constituents, molecular groups and structures, and polarity and nonpolarity behaviors of the molecules. These chemical properties govern the performance of asphalt. One behavior of asphalt that is very interesting to researchers and pavement professionals is viscoelasticity; at high temperature, asphalt is a viscous liquid, and at low temperature, it behaves like an elastic solid and becomes fragile. Chemical properties of an asphalt binder are also highly depended on the sources and processes employed.

2.1. Functional Groups and Chemical Families. Many chemistry-based techniques such as elemental analysis, Fourier transform infrared (FTIR) spectroscopy, gel permeation chromatography (GPC), thin layer chromatography (TLC), and high-performance liquid chromatography (HPLC) are commonly used in chemical characterizations of asphalt binders. For instance, as part of a comprehensive study of multiscale modeling, Stangl et al. [5] performed elemental analysis of an asphalt sample following the ASTM D5291-02 method, and some of the results are presented in Table 1. As indicated earlier, the chemical compositions of asphalt vary with the source of asphalt, processes adopted to manufacture it, analytic techniques utilized in elemental analysis, and chemical solvents and adsorbents used to obtain the compositional information. However, the variability among dominating elements such as carbon, hydrogen, and oxygen is less observed than that of foreign elements such as vanadium, nitrogen, and sulphur, as presented in Table 1. At a molecular level, researchers have proposed various structural models of asphalt. Such a structure for the strategic highway research program's asphalt sample (AAD-1 also known as California Coastal AAD-1) is presented in Figure 1, where a long chain of hydrocarbon along with some other chemical elements such as nitrogen and sulphur is modeled.

In the real world, asphalt binder interacts with a large number of environmental and mechanical factors such as oxygen, heat radiation, UV radiation, moisture, and traffic factor. These factors often act in a conjoint environment that affects the asphalt at the compositional, molecular, and macro levels. The consequential performance due to changes in chemical compositions and molecular structures should be taken in consideration when using the binder in a new pavement construction.

2.1.1. Molecular Groups of Asphalt. At molecular level, asphalt can be considered a complex organic compound consisting of groups of different molecules. Based on the size and polarity, they can be grouped as saturate, aromatic, resin, and asphaltene (often called SARA). Together they form a colloidal system—where asphaltene is a relatively stiffer and disperse domain, and later, three form a liquid substance that holds the asphaltene. The later three compositions are also called maltene. There have been many methods employed to better understand the characteristics of these fractionates and to quantify their share in asphalt. A rapid and inexpensive characterization method is thin-layer chromatography (TLC). This technique separates asphalt fractionates by some organic solvents. For example, asphaltene is precipitable by n-heptane where maltene dissolves, saturate by cyclohexane, aromatic by dichloromethane, and finally, resin by methanol or isopropanol [11, 12]. In this test process, a mobility parameter (R_f) for the fractionate is determined using a model, as shown in equation (1). Table 2 presents the approximate R_f value for four fractionates. However, R_f from one lab testing may not match with that of another since this parameter is also dependent on the sample size (thickness and diameter), solvent type, and so on, which are used in the characterization process. To obtain the SARA information, another method the so-called Iatroscan method that combines thin-layer chromatography and flame ionization is also employed frequently.

$$R_f = \frac{D_s}{D_m}, \tag{1}$$

where R_f = mobility paramter of the asphalt fraction, D_s = distance moved from point of application by solute, and D_m = distance moved from point of application by mobile size.

Technology has also made possible to physically visualize these fractionates. When a maltene fractionate is irradiated by an UV ray with an appropriate weblength, a chromatograph of maltene can be obtained, as shown in

Table 1: Asphalt chemical constituents and their share. The table is reproduced from Stangl et al. [5] (under the creative commons attribution license/public domain).

Asphalt state	Chemical constituents (mass %)					
	Carbon	Hydrogen	Oxygen	Nitrogen	Sulphur	Total
Neat asphalt (British specification B50/70)	83.90	10.40	<0.1	0.40	5.00	99.70
After RTFO	83.80	10.40	<0.1	0.40	5.00	99.60
After RTFO + PAV	83.70	10.50	<0.1	0.50	4.90	99.60

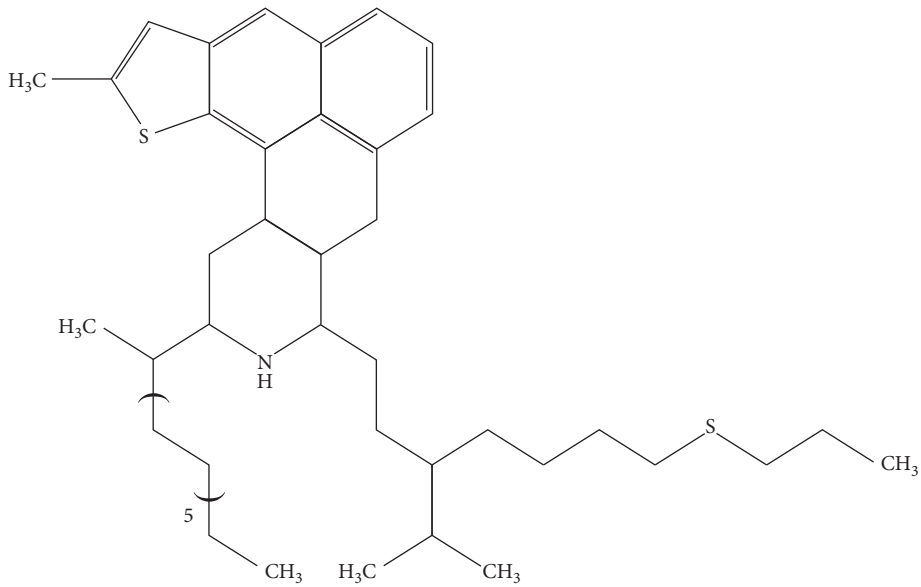

Figure 1: Average structure of California Coastal (aad-1) asphalt molecules. The figure is obtained from Lesueur [10] (under the creative commons attribution license/public domain).

Table 2: R_f value for asphalt fractions.

Asphalt fractions	R_f value
Asphaltene	0.20–0.21
Resin	0.45–0.47
Saturate	0.90–0.92
Aromatic (mono, di, or poly)	0.68–0.83

Figure 2(a). Physically, saturate (S) has yellowish color, and the color of aromatics (A) ranges from light yellow to light reddish based on polarity of the molecules, and finally resin (R) appeared as dark black color [14]. Figure 2(b) shows the Yen–Mullins model of asphaltene (AS). This model specifies that asphaltene can be present in bituminous materials as an isolated molecule or as a colony of six to eight molecules or clusters of about eight molecules. Figure 3 displays how a vital engineering property (in this case, viscosity) varies with SARA fractionates of an asphalt sample collected from California Valley. In a related study, Hofko [16] reported that among SARA fractionates, the asphaltene fractionate significantly influences the viscoelastic behavior of asphalt. Therefore, understanding of these fractionates in regard to chemical formation, behavioral characteristics, and, more importantly, engineering properties such as stiffness, creep, and viscoelasticity are critical and can be utilized to develop a model at microscale and thereafter to the full pavement model.

3. Morphological Models of Asphalt

3.1. Overview. Morphological studies deal with understanding of structural form of a matter, and they attempt to link the formation of the matter to its structural performance. To have a better understanding of morphology of a matter at microscale, a superior technology is needed. With the advent of new micro- and nanoscopic technologies, pavement researchers around the world added a rich amount of information on the body of knowledge in last two decades. Technologies used by researchers included, but not limited to, scanning electron microscope (SEM), florescence microscope, atomic force microscope (AFM), transmission electron microscope (TEM), and environmental scanning electron microscope (ESEM) with various advance engineering fixtures at different capacities. As previously mentioned, researchers now have been trying to connect this morphological information of asphalt binder to better predict the pavement performance over its design life.

In recent years, researchers predominately used AFM and SEM techniques. The AFM has some advantages and disadvantages over the SEM and vice versa. The AFM can provide three-dimensional morphological images of a binder sample, whereas the SEM provides two-dimensional images. The AFM sample preparation does not require a sputtering sample coating, which is required in SEM

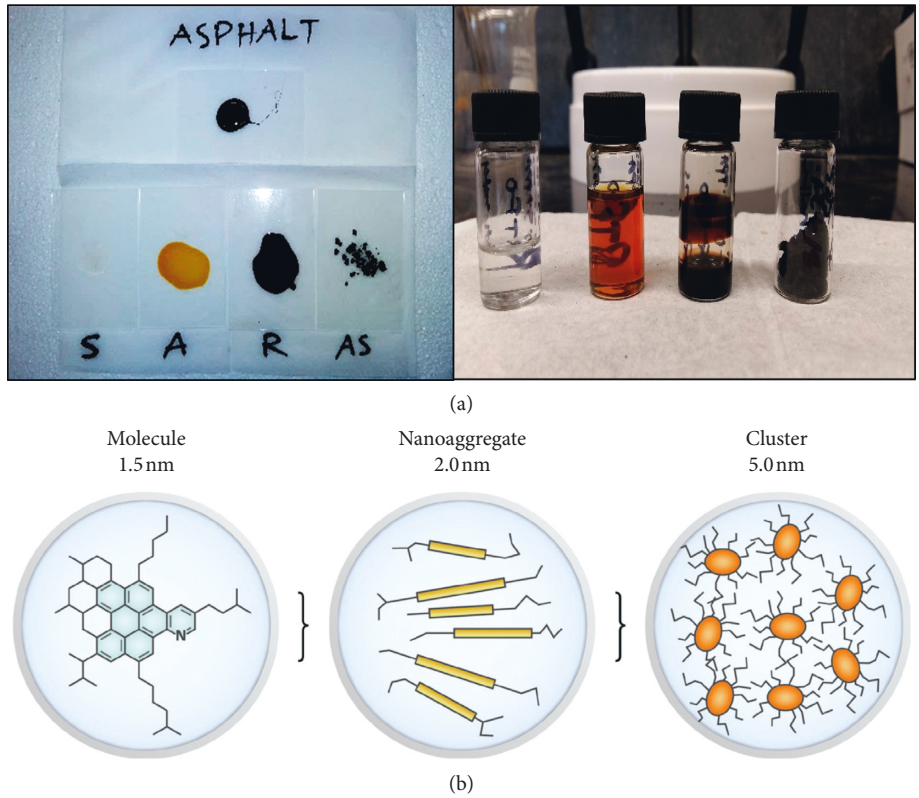

FIGURE 2: (a) Maltene (S = saturate, A = aromatic, R = resin), and (b) asphaltene (AS). The figure is reproduced from Mullins et al. (under the creative commons attribution license/public domain) [13].

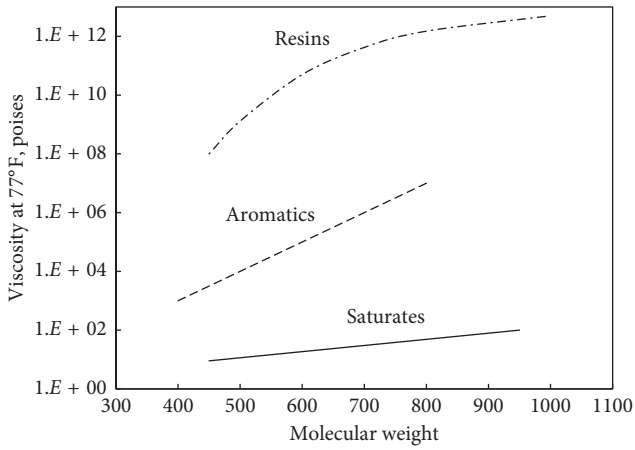

FIGURE 3: Changes in viscosity for different asphalt fractions under different molecular weights. The left figure is obtained from Griffin et al. (under the creative commons attribution license/public domain) [15].

analyses. A comparative advantage of the SEM is that it can image a large area (on the order of square millimeters), whereas the AFM can only image a maximum scanning area of about 150 × 150 micrometers. Furthermore, the scan rate of an AFM is relatively lower than that of an SEM. Figure 4 shows microscopic views of an asphalt sample under fluorescence [17] and atomic force microscopes. A pioneer study on asphalt morphology is conducted by Loeber et al. [18]. From inspecting these microscopic images, one can easily see that there is a circular kind of particles in a matrix system. The particles are of different sizes and are randomly placed within a couple of micrometers. Interestingly, these particles are available in both images obtained from two different microscopes that completely utilize different techniques; however, they still presented similar results in terms of sizes for the particles, orientation, and matrix design. For brevity, the current study is not focusing the techniques behind the different microscopes. Many studies also investigated the pattern, thickness, resistance force, deformation, stiffness, and other engineering properties of this circular domain in asphalt material, and that will be discussed in the following sections.

3.2. Analysis of Morphological Phases of Asphalt. It is generally believed that asphalt has three morphological phases (also called microdomains): a disperse phase, a relatively larger phase than disperse phase surrounding to the disperse phase, and finally a continuous phase. A better understanding of the engineering properties of these morphological phases of asphalt is expected to help scientists to develop better models for predicting pavement performance [19–22]. In a recent study, Pauli et al. [20] reported how the morphological phases affect microstructure of asphalt and how some external variables inherited to microstructure influence the morphology. Figure 5 shows images obtained through an AFM,

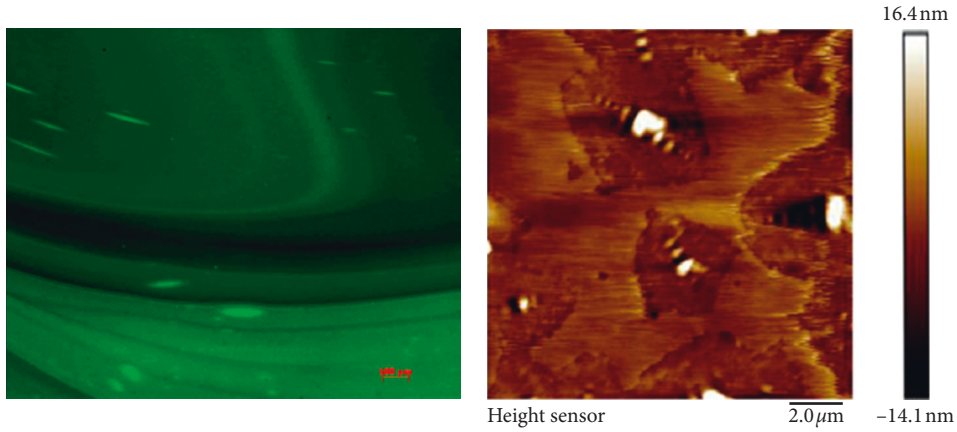

Figure 4: Asphalt sample view obtained from a fluorescence microscope on the left and an atomic force microscope on the right. The left figure is obtained from Kraus [17] (under the creative commons attribution license/public domain).

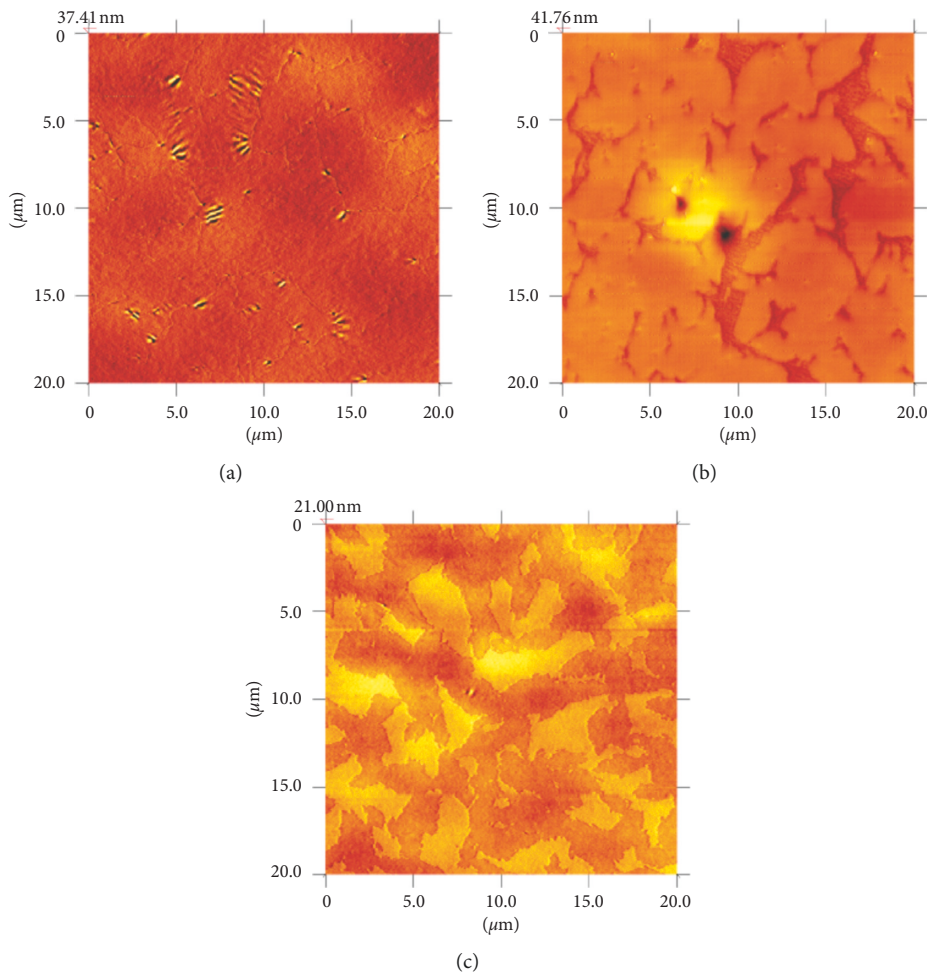

Figure 5: Images of asphalt morphology (AAK-1 sample, size 20 μm × 20 μm) of film thickness of 1600 nm (a), 1000 nm (b), and 600 nm (c). The figure is obtained from Pauli [23] (under the creative commons attribution license/public domain).

and it displays changes in morphological phases as a function of asphalt film thickness [23]. It can be seen that the disperse domain significantly varies as the sample thickness changes; the thinner the sample is, the lesser the presence of disperse domain is. However, some studies also concluded otherwise that the microstructure is independent of asphalt film thickness. Therefore, further research is needed to clarify this issue.

The disperse phase in the asphalt microstructure is considered as a "bee"-like structure with ridges and valleys within this phase. A bird's eye view of an AFM specimen of 15 μm × 15 μm can be seen in Figure 6(a), and details of this bee structure are presented in Figure 6(b), where the depth and spacing of valleys and ridge scan can be observed.

Some studies [25] named these three phases differently. The central part (disperse) within each highlighted area is also called the catana phase (so-called, bee), immediately around the catana phase is called the interstitial/periphase, and both of these phases are suspended from another phase called the perpetua phase or matrix (Figure 7). It has been reported that periphase and perpetua phase change with temperature; as the temperature increases, these phases interconvert from one to another, which has been observed in differential scanning calorimetry study by Soenen [26].

A few studies initially assumed a link on the relationship between the catana phase and asphaltene [18]. However, later other studies found this relationship is not statistically significant, while there is a highly plausible evidence that the catana phase is highly related to the presence of metal elements (e.g., nickel and iron) in the asphalt [24].

Menapace et al. [27] has investigated on the growth and height of the catana phase, and the study found that both are affected by the testing temperature in an AFM investigation. Table 3 presents that in general, the average diameter of bee structure increased as temperature increased for selected types of asphalt tested, and the same trend can be noticed for the area covered by the bee structure phase for one asphalt grade (PG 76-22), whereas a mix result was observed for another asphalt grade (Pen 60/70). The increased size of "bee structure" could be due to the disintegration of bees due to increased temperatures. Allen et al. reported that the dispersed phase (i.e., bee) increased as saturate fractionate in the asphalt increased [28]. The dispersed phase can completely change when a virgin asphalt is mixed with aged asphalt binder from either recycled asphalt pavement or roof shingles; microparticles found in the interfacial zone ranged from 160 nm to 2.07 μm by recent multiple studies [29, 30], as presented in Figure 8 [31].

All these research results suggest that asphalt binder has complex phases, which are influenced by many experimental and environmental factors. However, if we can obtain generalized information on these phases and if they are based on good amount of data, a link can ultimately be developed between microcharacteristic and macrolevel pavement performance.

Soenen et al. [25] reported that morphologies of the asphalt sample are highly influenced by the temperature employed to prepare the sample, the elapsed time in that temperature after isothermal condition reached, and other experimental factors. Surface morphologies changed in terms of network structural forms and sizes between the samples when tested at an isothermal condition for different temperatures (Figure 9). Perhaps, this is why, asphalt binder's rheological performance changes due to thermal aging.

3.3. Effect of Aging, Additives, and Rejuvenators on Asphalt Morphology. When asphalt is utilized in real-world applications (e.g., pavement), it experiences a very complex environment throughout its life. Some major chemical compounds or environmental factors that asphalt interacts with are atmospheric oxygen, dissolved oxygen, UV radiation, and other hundreds of known and unknown solid, liquid, and gaseous compounds. As a consequence of the interactions between asphalt and surrounding chemical compounds, asphalt loses its some vital rheological properties over time, which is termed as aging of asphalt. Many researches have been conducted to mimic the aging processes in laboratories, to model field aging and finally to deter aging by using additives such as polymers and rejuvenators. Two aging processes for asphalt binder are commonly employed in laboratory testing: one is the rolling thin-film oven test (RTFOT) process to simulate preservice aging and other is the pressurized aging vessel (PAV) process that simulates in-service aging.

Figure 10 shows that the catana phase is very dominant in an aged sample than that of an unaged sample, indicating significant differences in the phase angle (i.e., higher changes in elevation) between disperse domain (catana) and continuous matrix (peri and perpetua). Moreover, the percentage of area covered by disperse domain reduces significantly with the PAV process compared to the RTFOT aging. To better understand the engineering properties of these phases for "before" and "after" aging conditions, Allen et al. [32] conducted a comprehensive research study on the subject matter and developed an improved technique to obtain microrheological property of the phases such as creep information of asphalt fraction morphologies. This study reported that the creep was affected by the aging and can be noticed in Figure 11. The asphalt binder sample shown in Figure 11 is a SHRP's AAD sample. In this figure, Phases 1, 2, and 3 refer to catana, peri, and perpetua phases, respectively.

In Brazil, Rebelo et al. [34] recently investigated on how RTFOT and PAV processes affect the morphologies of asphalt using an atomic force microscope. These researchers reported that there was no catana phase observed in the sample after both aging processes. Interestingly, these researchers did not see the catana phase before aging the sample too. Figure 12 presents the topographic and phase contrast images of asphalt sample with various recycled binders (RAP) after different aging conditions. The lateral dimensions of the AFM-based images shown in Figure 12 are 10 μm × 10 μm. The scale of the topography images is 20 nm. Absence of the catana phase in the unaged sample is not new. For example, the study conducted by Qin et al. also supports the observation of the Rebelo study [35]. In addition to thermal and oxidative effects on asphalt binder, various forms of moisture precipitate from atmosphere also damage asphalt pavement significantly. Dos Santos et al. [36] reported that the catana and perpetua phases are significantly affected by moisture that, in turn, affects the rheological and adhesive properties of asphalt binder.

In the recent years, to improve pavement performance, the addition of different polymers or additives in asphalt binders has become a common practice in the industry. In

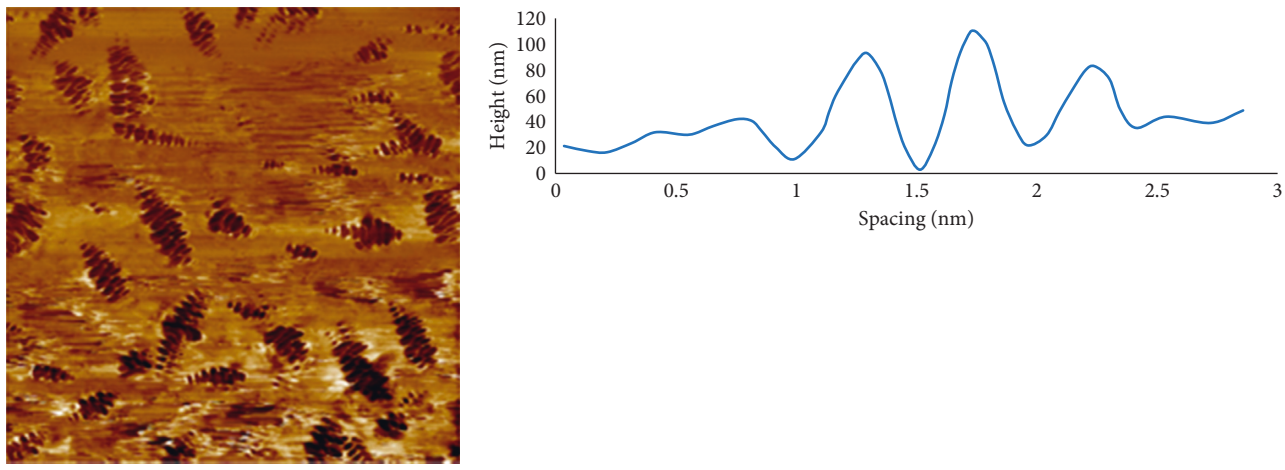

Figure 6: (a) A bird eye view of asphalt sample under AFM, and (b) a tentative topographic profile of bee structure. The Figure 6(b) is reproduced from the data reported by Masson et al. [24] (under the creative commons attribution license/public domain).

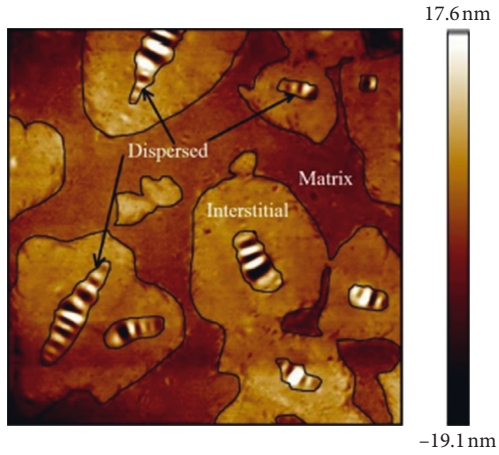

Figure 7: A detail view of all morphological phases in asphalt.

Table 3: Effect of temperature on diameter and area coverage of bee structure in asphalt. The table is reproduced from Menapace [27] (under the creative commons attribution license/public domain).

Treatment temperature	Pen 60/70		PG 76-22	
	Average diameter (μm)	% area covered	Average diameter (μm)	% area covered
Room temperature	0.27	22	0.27	35
50°C	0.58	56	0.56	53
70°C	1.07	66	0.99	60
100°C	1.64	55	2.06	63
130°C	1.54	51	2.13	69
150°C	1.48	43	1.83	60

microstructure investigation, it was found the addition of polymer basically changes the microstructure of the original binder, and the improvement in modified binder in regard to rheological or adhesive property is strongly associated with changes in microstructure or new morphologies developed in the modified binder [35, 37, 38]. Another study [25] also reported that asphalt morphology is influenced by the UV aging.

The main consequence of various aging is formation of crack in asphalt. Researchers have been trying to use a rejuvenator in a capsule (very fine shell) during pavement construction. The idea is when a microcrack initiates and passes through randomly spread rejuvenator shells, the shell breaks and liquid rejuvenators spread in the microcracks [39]. Morphologies of asphalt with asphalt modifiers and closer view of the cracks has been shown in Figure 13. Depending on morphologies of the crack surfaces, appropriate rejuvenators can improve both adhesive and cohesive bond properties of asphalt binders, and thereby crack propagation is deterred. All of these studies strongly demonstrate the strong association between the morphological properties and microstructural performance of asphalt. The authors also believe that the understanding of this association can be linked to macrolevel performance of the pavement in the real world.

3.4. Network Structure of Asphalt Molecules. To better understand the architectural pattern, i.e., the design of network of molecular compounds and how the network is associated with asphalt binder's fundamental properties (e.g., adhessibility and stiffness), a few studies have been done. To capture the network design of asphalt molecules, electron micrograph drawn by utilizing scanning electron or environmental scanning electron microscopes is common in the literatures. Between these two systems, literatures have come to a point that, to realize the goal of understating of surface network morphology, the environmental scanning electron microscope does a better job than that of scanning electron. In the latter technique (i.e., scanning electron), an asphalt sample is distorted by the evaporation of some hydrocarbon molecules with the heat radiated from the electron beam [41]. To avoid the evaporation of some molecules, thereby, maintaining the integrity of the testing sample, a carbon coating on the sample is done when a scanning electron microscope is utilized in network structure study. However, this takes meticulous sample preparation efforts and

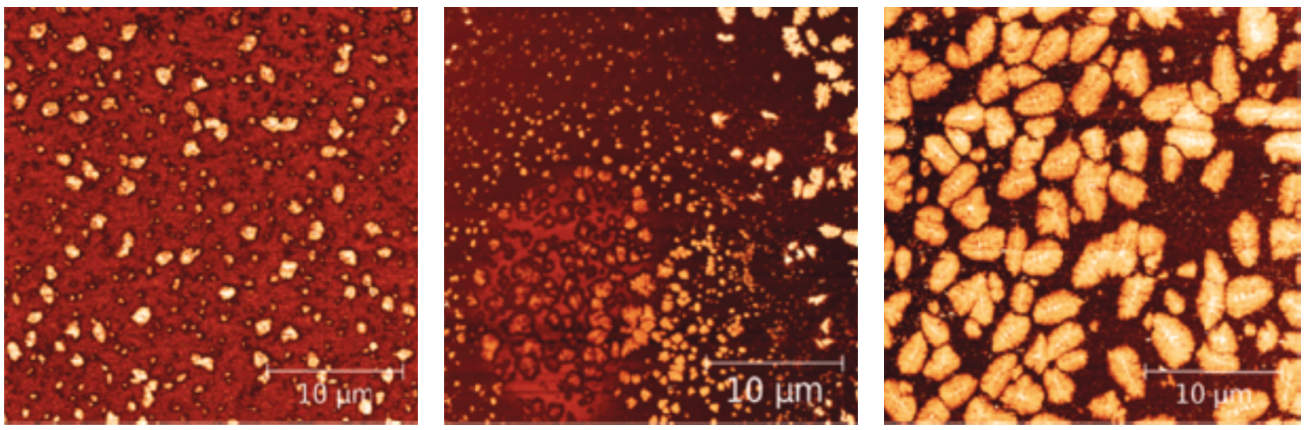

(a) (b) (c)

Figure 8: (a) Micrographs of RAP asphalt binder, (b) RAP and virgin asphalt binder's interfacial zone, and (c) virgin asphalt. The figure is obtained from Nahar [31] (under the creative commons attribution license/public domain).

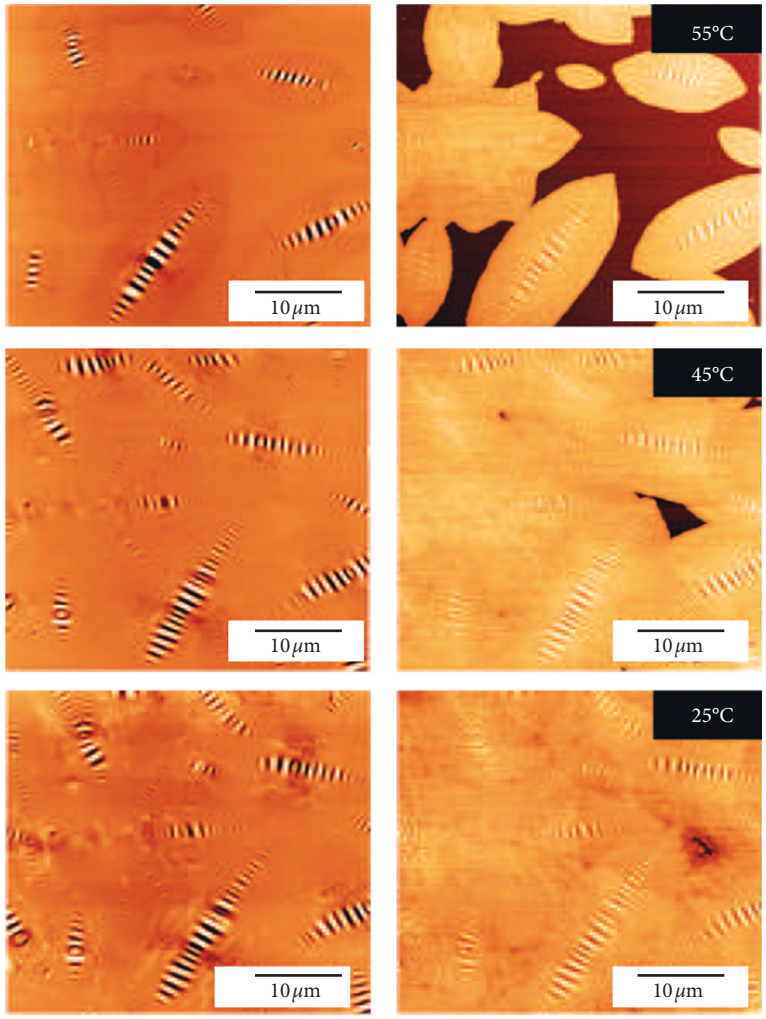

Topography Phase

Figure 9: Microscopic images of asphalt morphologies under different temperatures. The figure is obtained from Nahar [31] (under the creative commons attribution license/public domain).

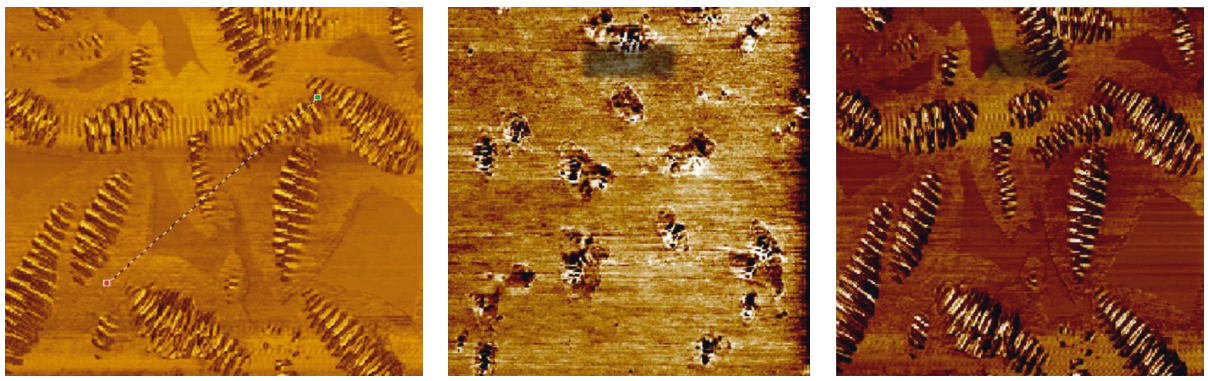

(a) (b) (c)

Figure 10: (a) AFM micrograph of asphalt showing catana, peri, and perpetua phases, (b) micrograph before aging, and (c) micrograph after aging. The figure is obtained from Allen [33] (under the creative commons attribution license/public domain).

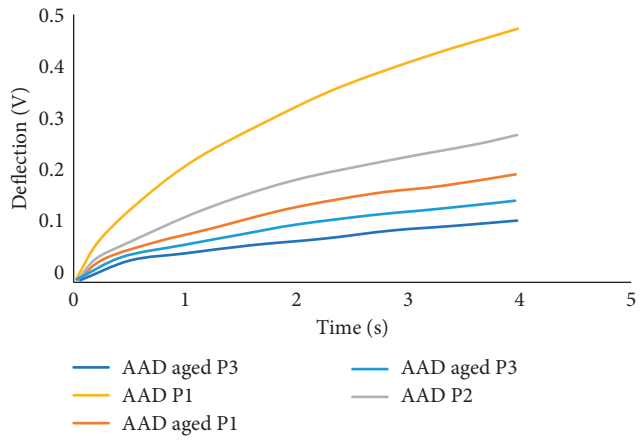

Figure 11: Effect of aging on asphalt phases. The figure is obtained from Allen et al. [33] (under the creative commons attribution license/public domain).

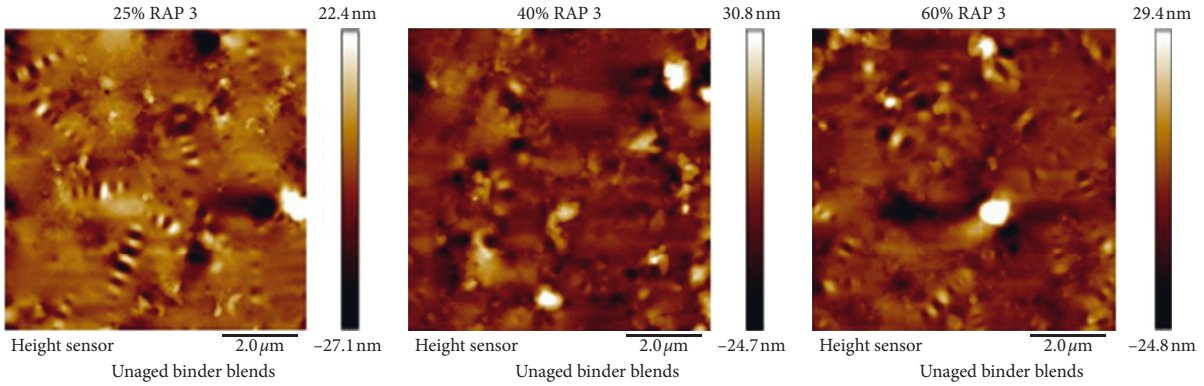

(a) (b) (c)

Figure 12: Continued.

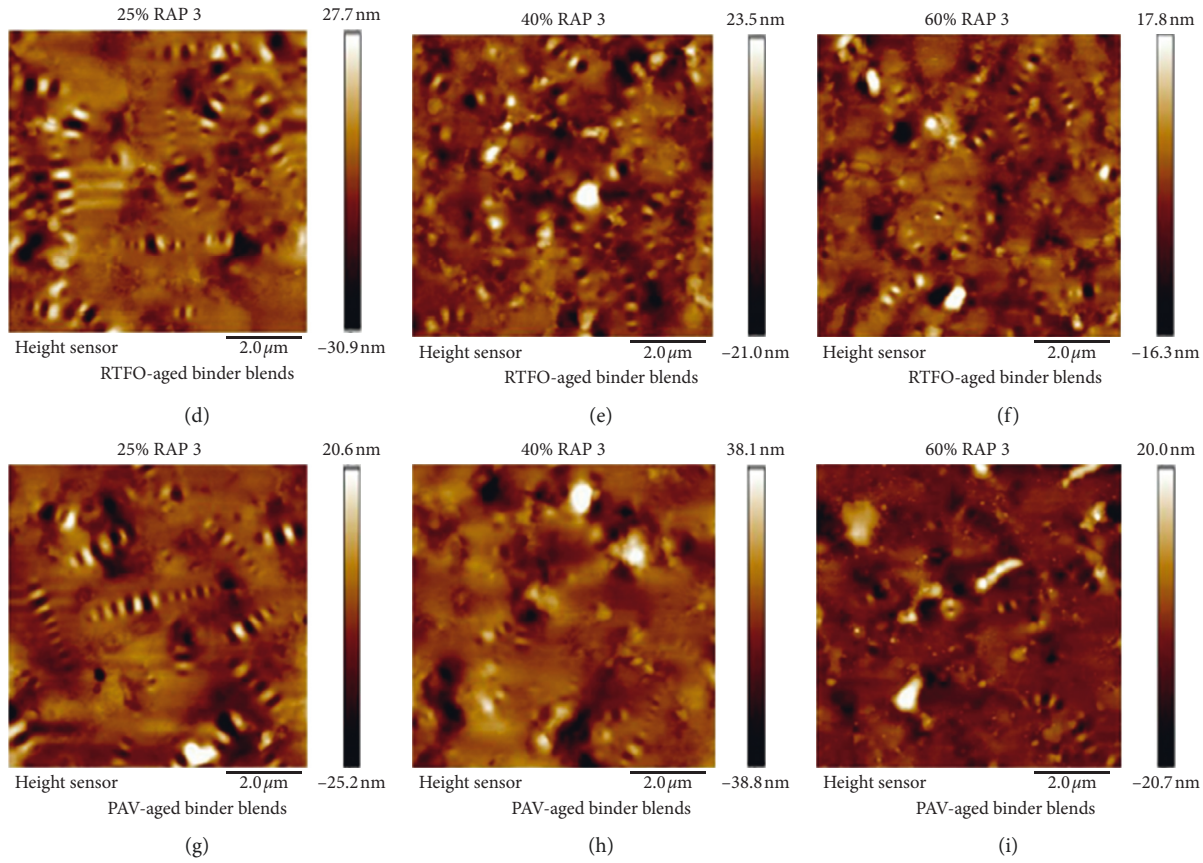

Figure 12: Morphology of RAP-asphalt blends: (a–c) 25%, 40%, and 60% unaged blends, (d–f) 25%, 40%, and 60% RTFO-aged blends, and (g–i) 25%, 40%, and 60% PAV-aged blends, respectively.

extended time to test [42]. Detail information on how these microscopy works and advantages and disadvantages are available in [43].

Figure 14 shows micrographs of asphalt binder's molecular network captured by an environmental scanning electron microscope [44]. A network entanglement that consists of thousands of rope-like elements (also called network strand or fibril) can be observed. The average diameter of this fibril is reported 10 micrometers for an unaged sample [45]. But, when an aged sample was tested, observed fibrils were found to be a bit coarser than that of an unaged sample. Rozeveld et al. [42] also investigated the network structure of asphaltene fraction (phase with heavy molecular weight) after fractionating by n-heptene and reported the presence of a network of interconnected lentil-like particles than a network of smooth fibrils. This individual chemical family (asphaltene fractions) had an average size of 0.2 to 0.3 micrometer before aged, whereas after aged, the fractions became significantly larger in size (0.8 to 1.2 micrometer). The increase in size was attributed to the change in molecular structure by oxidation during aging. The observation made by Khattak et al. [46] supported the findings of Rozeveld et al. [42], which reported a network of interconnected lentil particles (asphaltene particles). The study [45] also included time-dependency effect on network design in their experimental matrix. Interestingly, distinct differences in the network structure were observed for different level of interaction between asphaltene molecule group and n-heptane, as can be seen in Figure 15 [47].

Figure 16 shows an ESEM image of asphalt sample tested under irradiation loading [44]. When the asphalt sample is loaded under tensile loading, the fibril network was found well aligned [42]. This observation suggests that when asphalt is loaded, the fibril network provides the resistance force and that ultimately help contribute to prevent deformation, and, also possibly, the fibrils act as a stitching between the microcracks and participate to reduce crack propagation under the loading. Some studies also reported that the network structures were changed with the addition of polymer and its dosages (Figure 17) and indicated that rheological properties and microperformances changed after the addition of polymers could be linked to the modified network of the fibrils [11, 42, 48]. Similar observations were made by some other researchers who compared the morphological structure of a neat asphalt and the asphalt binder modified with carbon nanofibers. However, this was not the case for the study conducted by Stangl et al. [5]; this group did not find any significant difference between the network structures with and without polymer modification of asphalt binders. The effects of aging on network structure were observed significant, only after long-term aging (PAV) in the Stangl et al. study [5], however other study reported aging changed asphalt ESEM profiles as tested for different temperature and duration, as displayed in Figure 18. To be

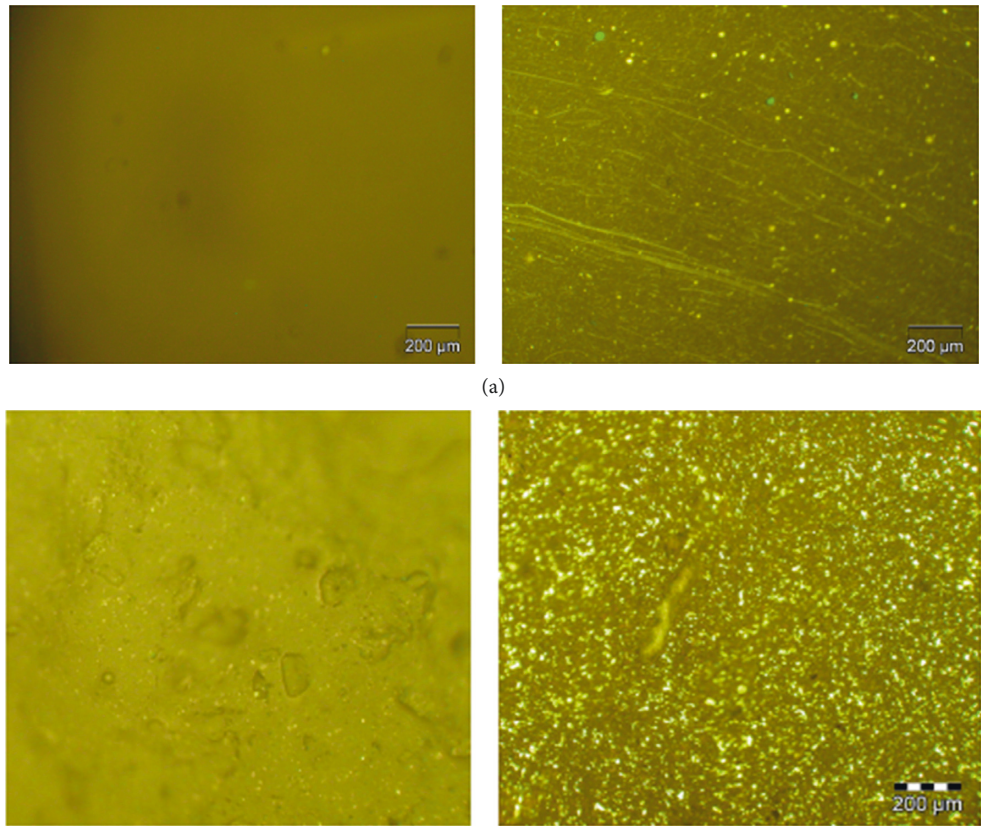

(a)

(b)

Figure 13: (a) Fluorescence microscopy of pure bitumen (left) and SBS modified bitumen (right). (b) Fluorescence microscopic pictures of the cross section of the PBmas (left) and the SBSmas (right) directly after being broken at 0°C. This figure is obtained from Qiu [40] (under the creative commons attribution license/public domain).

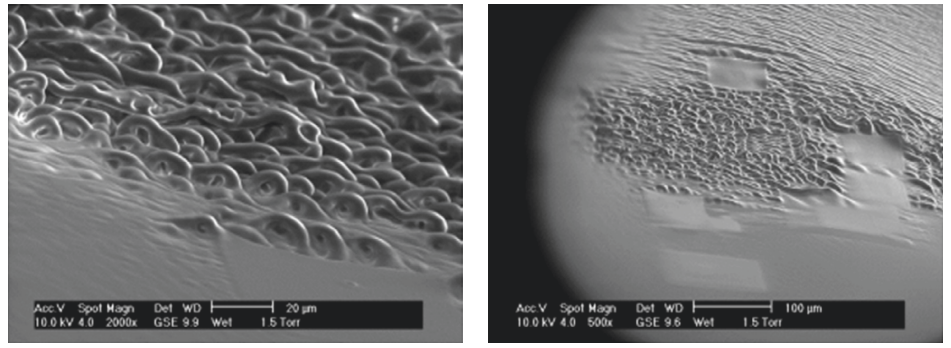

(a) (b)

Figure 14: (a) Micrograph of an asphalt sample after 2 minutes irradiation. (b) Electron effects in that asphalt due to double irradiation. The figure is obtained from Gaskin [44] (under the creative commons attribution license/public domain).

precise, little to no change was noticed in the RTFOT sample, a contrast to the Shin et al.'s study [45] which suggests that a systematic standard test method for aging effect needs to be developed for improving reproducibility, which can be utilized to predict micro level performance with statistical reliability. Thus, results from micro- or nanolevel investigation can be helpful and can be connected to pavement-level model—a driving force of this review.

4. Micromechanistic Characteristics of Asphalt

This section summarizes micromechanistic characteristics and performances of asphalt binders and how they are influenced by chemomorphological properties that have been previously presented. Among many fundamental properties of asphalt binders, adhessibility, elastic and composite moduli, creep and deformation behavior, and

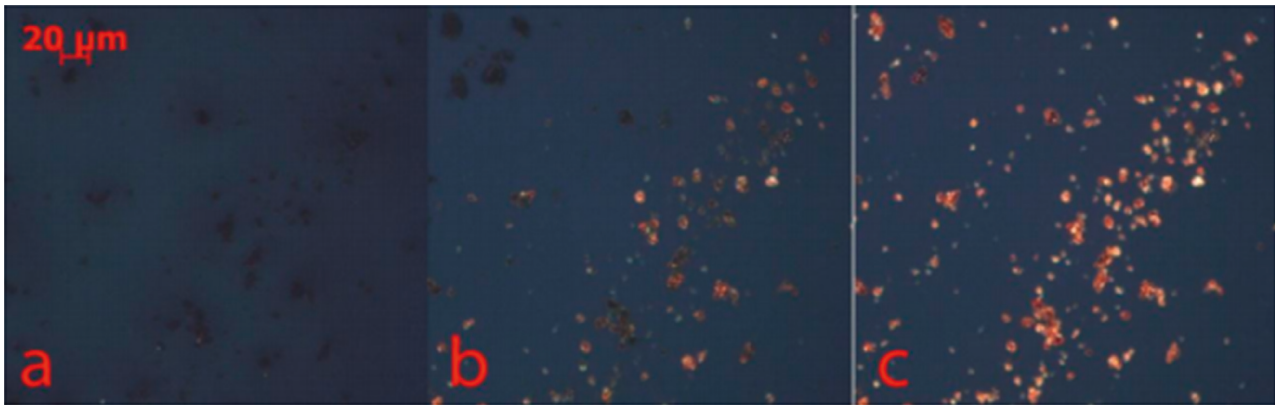

Figure 15: Topographic images showing the interaction between n-heptane and asphaltenes. (a) Asphaltene with n-heptane, (b) asphaltene during n-heptane evaporation, and (c) asphaltene after evaporation of n-heptane. The figure is obtained from Nikooyeh [47] (under the creative commons attribution license/public domain).

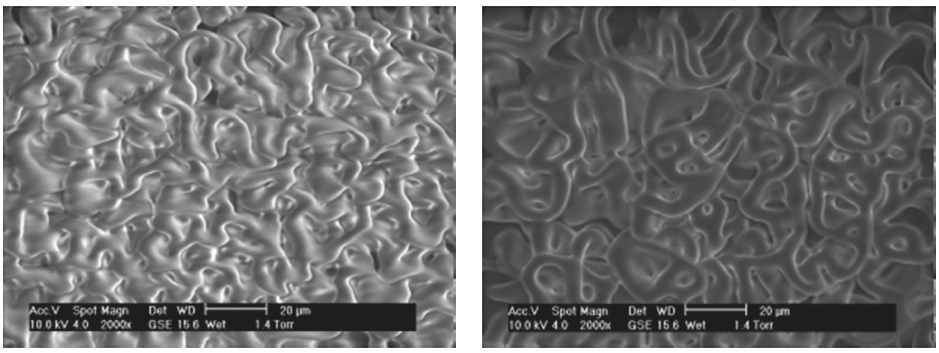

(a) (b)

Figure 16: Figure micrograph of maltene fraction after irradiation for 1 minute (a) and after 2 minutes (b). The figure is obtained from Gaskin [44] (under the creative commons attribution license/public domain).

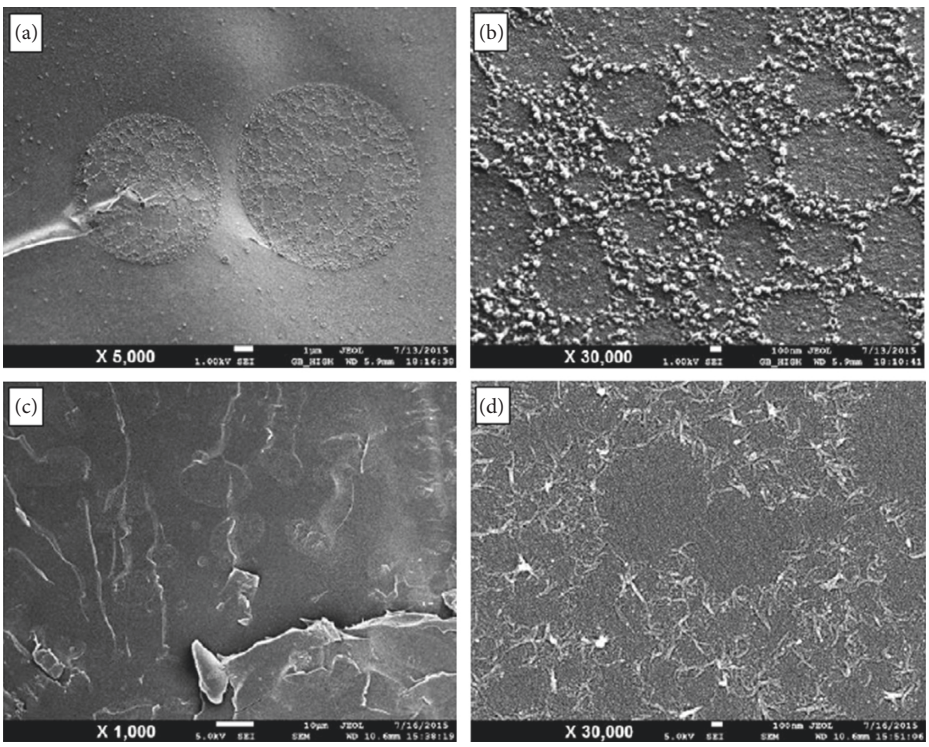

Figure 17: ESEM scan of modified asphalt (3% SBS) (a) 5000x and (b) 30000x. ESEM scan of modified asphalt (5% SBS) (a) 5000x and (b) 30000x. The figure is obtained from Jasso [48] (under the creative commons attribution license/public domain).

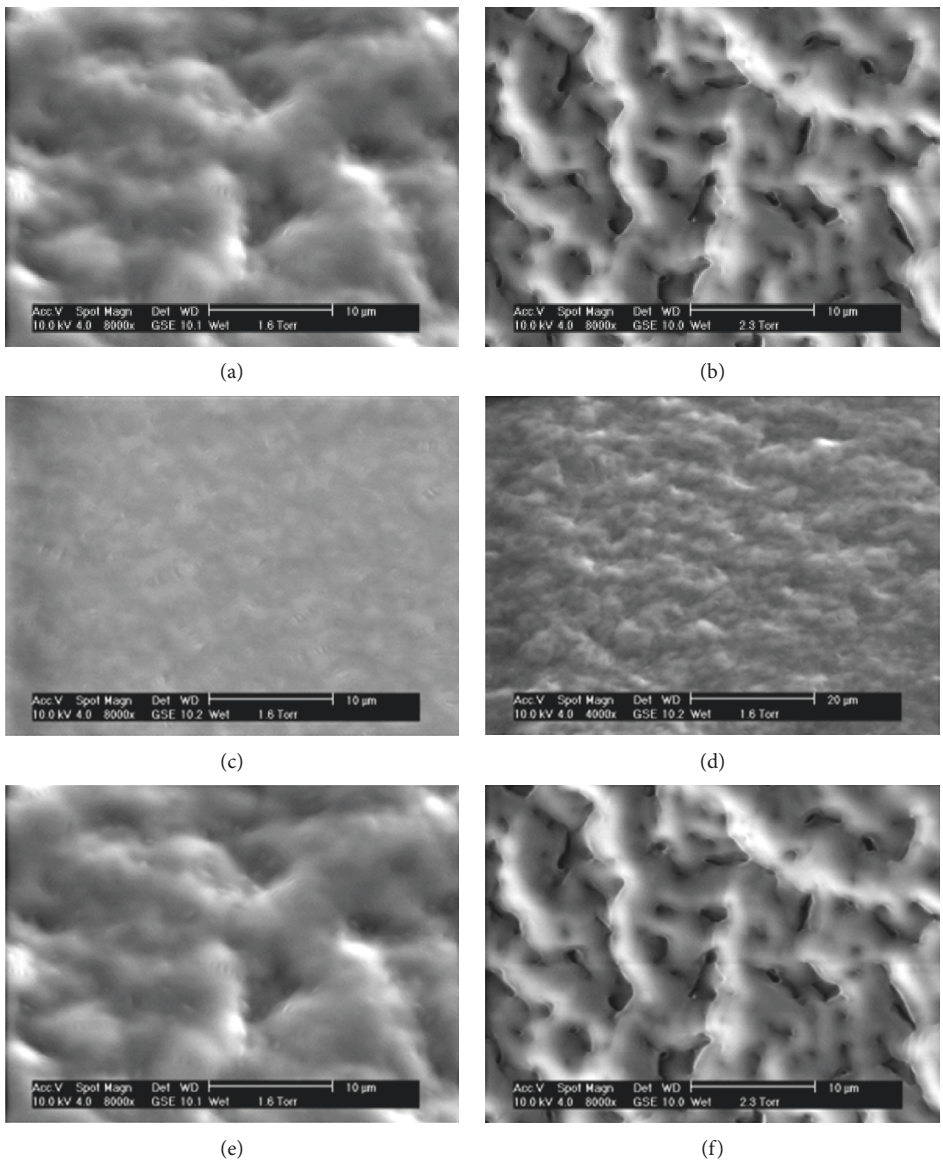

Figure 18: (a) ESEM profile of asphalt after aging at 0°C for 2 minutes, (b) after aging at 5°C for 2 minutes, (c) 10°C for 2 minutes, (d) 15°C for 2 minutes, (e) 20°C for 2 minutes, and (f) 25°C for 2 minutes. The figure is obtained from Gaskin [44] (under the creative commons attribution license/public domain).

frictional properties are often considered critical by the pavement community, and they are discussed in the following sections.

4.1. Adhessibility of Asphalt Phases. A number of studies have attempted to investigate the adhesion property of asphalt binders and their various microphases [49–55]. The adhessibility of an asphalt binder is found to significantly vary with asphalt source, chemical compositions, and types, and they are influenced by environmental factors such as temperature and moisture. These studies reported that the aforementioned factors also influence the adhesive force of various microphases of asphalt binders. In micro- and nanoscales adhesive force is estimated from the force-distance curve obtained in experimental results of the atomic force technique—the PFQNM™ (PeakForce quantitative nanomechanical) property mapping. In the PFQNM™ technique, the Derjaguin–Muller–Toporov (DMT) model, shown in equation (2), is utilized to predict adhesive forces. Detail technique can be found in many literatures [21, 40]. Figure 19 presents the variation of adhesion force within a 20-micrometer square asphalt fraction. In Figure 19, regions with white patches exhibiting bee structure (catana phase) have the weakest adhesive force than other phases. The color variation indicates force differences from none to about 242 nN. However, studies [55] found that, in general, some phases of asphalt have a distinctive pattern of adhesion forces. Figure 20 shows a tentative height profile indicating adhesion force over the profile of an asphalt sample. In general, the catana phase has the weakest adhesive force, while periphase has the highest adhesive force as reported by

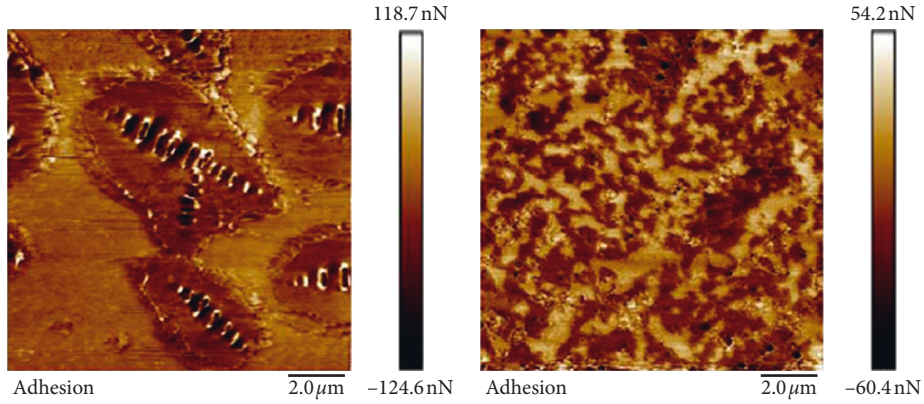

Figure 19: Micrograph of asphalt showing adhesion force overlay on a 20 × 20 micrometer sample.

Fischer et al. [49]. However, the third phase (perpetua) can exhibit adhesive force as high as periphase.

$$F_{\text{Adh}} = F - \frac{4}{3}E^{\text{r}}\sqrt{R\left(d - d_0\right)^3}, \tag{2}$$

where F_{Adh} = adhesion force, F = applied force, R = radius of the curvature developed due to the force, $d - d_{\text{o}}$ = deformation of the sample, and E^{r} = Young's modulus of the sample.

Within the catana phase of an asphalt binder, Dourado et al. [52] found that the adhesion force is very consistent; to be precise, the data had just a coefficient of variation of 16%. After conducting studies on a number of asphalt samples, Yu et al. [51] found that there was a statistically significant difference in adhesive force between two areas (raised and recessed) in asphalt, as shown in Figures 21(b) and 21(c). Chemomechanical properties of these morphological regions in the sample may be accounted for this difference are critical and needed to be better understood if adhessibility is sought to be enhanced for improving pavement performance. And, indeed, some improvement in adhesion force was noticed at nanoscale where the sample studied was modified by some hydrocarbon additives that can be seen in Rebelo's study [22]. Also, Tarefder et al. [56, 57] found this adhesion force enhancement occurred, in general, when asphalt was modified with common styrene-butadiene (SB), SBS polymers, and limes.

4.2. Modulus Behavior of Asphalt Micro Phases. With the development of the PFQNM technique in atomic force microscopy, it became possible to obtain nanomechanical properties of asphalt, on top of topographic height profile. Among three morphological phases discussed earlier, Fisher et al. reported that the periphase surrounding the catana phase is stiffer than the perpetua phase (smooth matrix), and the perpetua was found more viscous than the periphase. In this investigation for the modulus profile of an asphalt sample, two groups of moduli were noticed clearly: one group with a low modulus value, ranging from 300 to 450 MPa and the other group with a high modulus value, ranging from 500 to 750 MPa. It was also reported that low modulus zone corresponds to the perpetua phase while the high modulus zone corresponds to both catana phase and periphases [49]. Similar observations were made in the Lyne's work [55]. Surprisingly, later some other researchers [50] found that the perpetua phase had a higher DMT modulus value than that of peri/catana phase using (Figure 22).

Dourado et al. estimated elastic modulus of an asphalt sample on five different spots, which were mostly selected in bee areas [52]. Those spots were tested with varying loads ranging from 10 nN to 40 nN. Elastic moduli in these spots were estimated with equation (3), and it was observed that moduli values varied from 0.29 GPa to 2.0 GPa, with trend of the higher the load, the lower the modulus value, an opposite trend that is generally seen at a macroscopic scale. The perpetua phase (smooth matrix) was noticed to be stiffer than the catanaphase/periphase that supports Hossain et al.'s findings [50].

Allen et al. [58] examined viscoelastic/composite moduli of asphalt phases for aged and unaged conditions. A significantly higher modulus value was reported for all three phases in aged asphalt sample than that of the unaged sample. When an additive is added to modify an asphalt binder to improve its mechanistic behavior, the additive changes its morphological network as discussed in the previous section. In turn, the modified morphology helps improve the mechanistic performance. Such behavior was also seen in the microscopic scale—in terms of modulus of the asphalt phases. Besides, modulus values of asphalt phases in this very small scale is also significantly affected by the testing temperature. As expected, moduli of asphalt phases decrease as temperature increases, in general. Figure 23 presents a two-dimensional model and shows how modulus of catana, peri, and perpetua phases changes under a wide range of temperature.

$$E = \frac{4\left(1 - \vartheta^2\right)F_{\max}}{3\,\delta_{\max}^2\tan\alpha}, \tag{3}$$

where E = elastic modulus, F = maximum applied force, α = half angle in the tip of cantilever in atomic force microscopy, δ = indentation depth, and ϑ = Poisson's ratio.

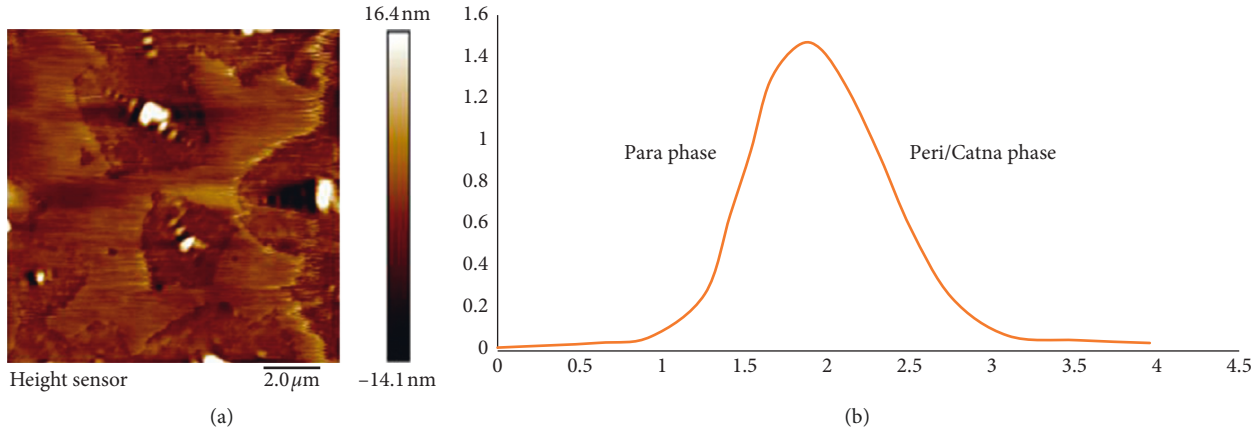

FIGURE 20: Different phases exhibit different adhesion force in the left image (a). Frequency distribution of adhesion forces (b). The Figure 20(b) is reproduced from Fischer et al. [49] (under the creative commons attribution license/public domain).

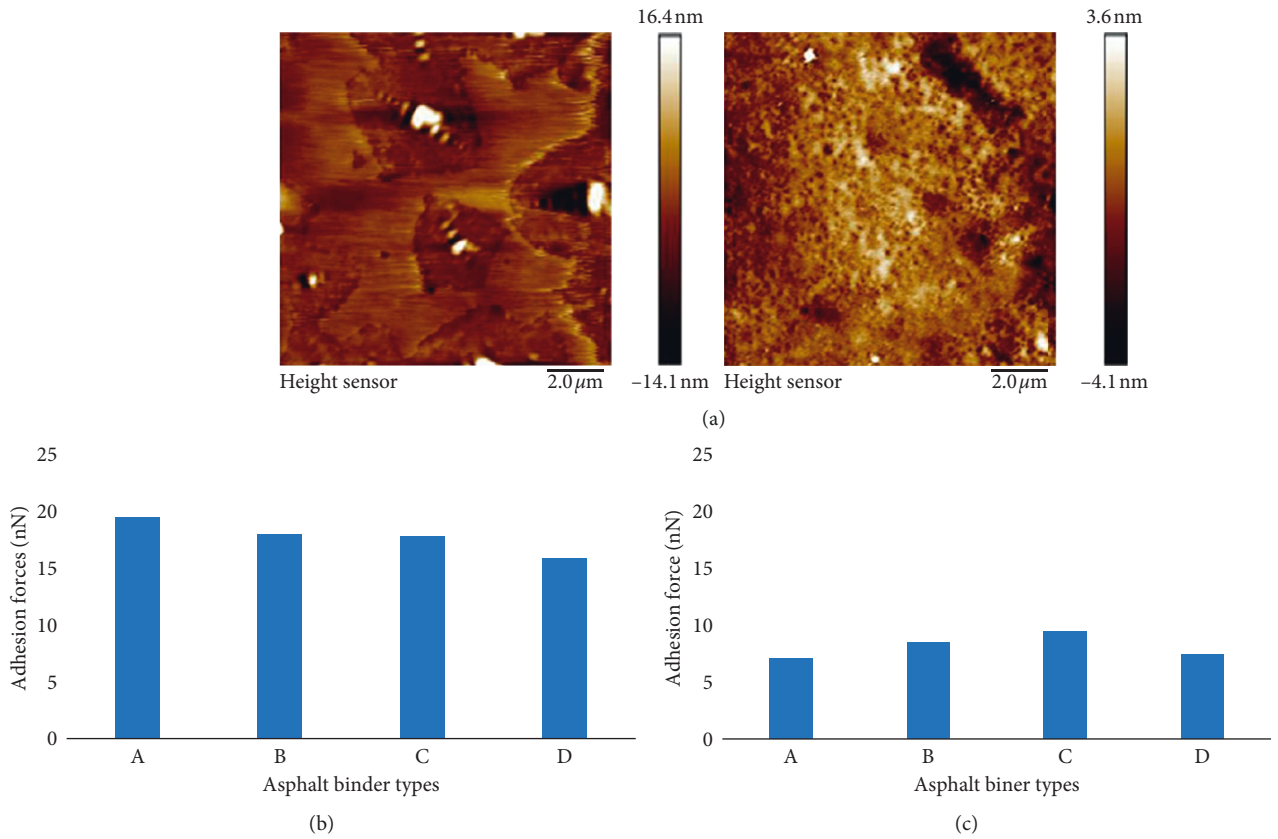

FIGURE 21: (a) Topographic image of asphalt sample with varying height, (b) adhesion force values (in nN) obtained in raised area from different samples, and (c) adhesion force values (in nN) obtained in recessed area. The Figures 21(b) and 21(c) is reproduced from Yu et al. [51] (under the creative commons attribution license/public domain).

4.3. Creep and Deformation Characteristics of Asphalt Phases. Asphalt is fundamentally a viscoelastic material—exhibiting the behavior of an elastic solid and a viscous liquid. When it is placed under a mechanical loading, it deforms instantly and also over time. When load is removed, some part of the deformation rebounds. Many studies have been conducted to understand this viscoelastic behavior of asphalt from micro- and nanoscopic scales [19, 35, 50, 52, 58]. Dourado et al. [52] examined how asphalt's morphological surface changes under mechanical loading (10 nN) over time with the AFM technique. It was reported that, after 12 minutes from loading, a dark zone appeared that reflected changes in morphology for an imposed load, but it is reduced significantly after an hour. Qtaish [59] also found similar results (Figure 24). Figure 25 displays how the phase deformation changes over time. Clearly, it can be noticed first

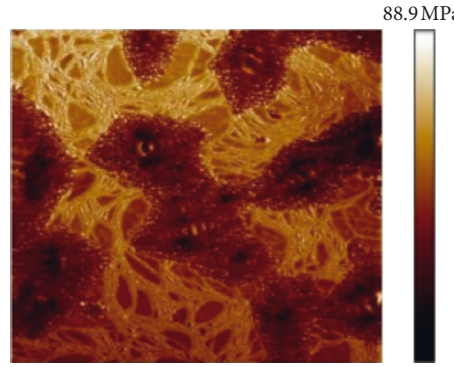

Figure 22: Modulus profile of an asphalt sample of 20 × 20 micrometer.

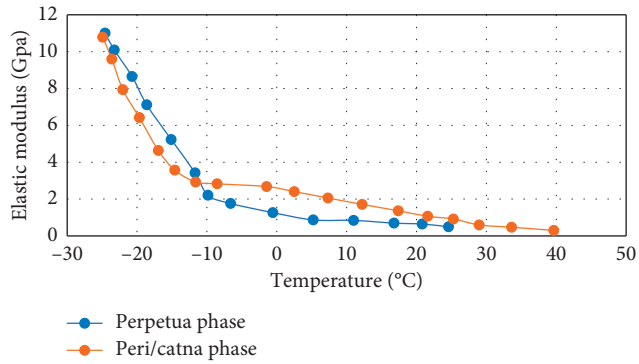

Figure 23: Effect of temperature on asphalt phases. The figure is reproduced from Fischer et al. [49] (under the creative commons attribution license/public domain).

deformation was increasing under the loading that could be attributed to the tensile effect on the surface, whereas after reaching the peak deformation, it decreased over time that can be attributed to elastic recovery after the load is removed.

Allen et al. [33] estimated deformation characteristics of asphalt phases for aged and unaged conditions for different asphalt samples and found different creep performance between the asphalts. Figure 26 shows deformation profiles of two phases (continuous phase/smooth matrix and dispersed phase/surrounding of bee) of SHRP ABD asphalt. For the unaged sample, higher deformation was observed in smooth matrix than the dispersed phase under a creep static loading of 5 nN, while almost similar deformation trend was observed for both phases in the aged sample, suggesting morphological changes of the phases during aging processes. Interestingly, aged phases exhibited an elastic solid material behavior—a linear deformation with time while unaged phases showed a lag in deformation response for the creep loading. Study also found that the deformation value of asphalt phases, that is critical for understanding nucleation of microcracks and developing prevention mechanisms, is changed with the additives added for asphalt modification or when a neat asphalt is blended with aged asphalt from recycled pavement [50]. Figure 27 shows asphalt phases after straining. Crack is nucleated around the bee areas at different scales and with different geometrical blocks—such differences can be attributed to the heterogeneity in the asphalt phases that induce differential local stress and strain with various amplitude leading to microcracks.

5. Concluding Remarks

Asphalt binder is a vital component for asphalt pavement and dictates the overall performance of pavement. Much research studies have been done to better understand the behavior and properties of binder. In the recent years, a number of studies have also been conducted to understand asphalt binder at molecular/nanoscale level. A thorough review on asphalt binder's binder properties at different scale levels has been conducted in this study. Based on the review of the literature, the following can be concluded:

(i) To better understand and predict the performance of pavement, it is important to understand the behavior and performance of asphalt binder at molecular and nanoscales. This became even more important with the increased trends in modification of asphalt binders and utilization of recycled asphalts in new pavement constructions.

(ii) Asphalt molecular models are widely varied depending on origins, chemical processing, and so on.

(iii) At the nano level, an asphalt binder has three major microdomains: catana phase (also called dispersed

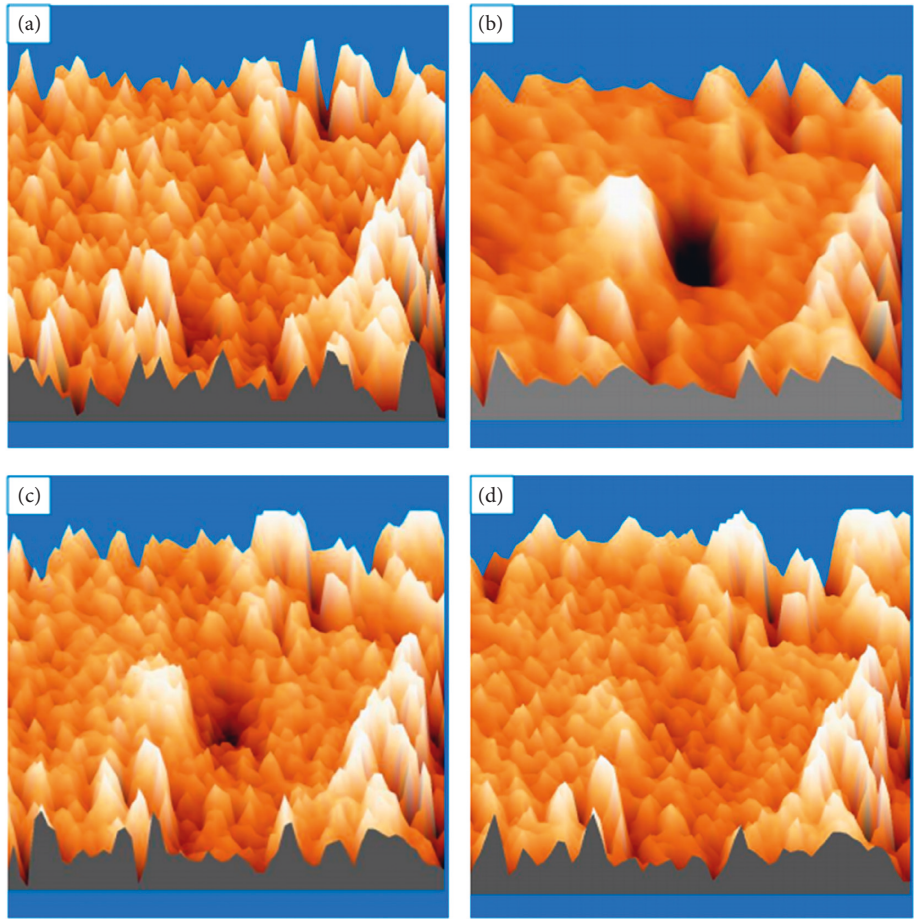

Figure 24: Asphalt micrograph: (a) directly before loading, (b) 163 sec after loading, (c) 350 sec after loading, and (d) 800 sec after loading. The figure is obtained from Qtaish [59] (under the creative commons attribution license/public domain).

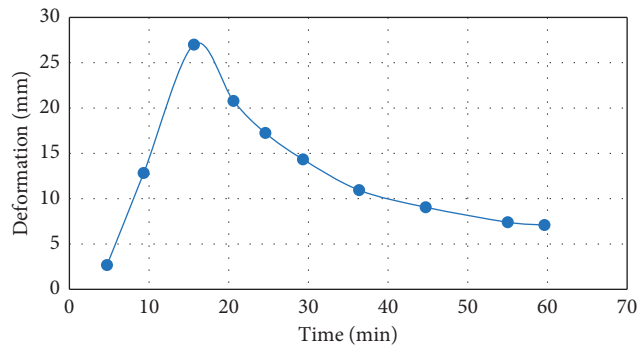

Figure 25: Changes in deformation in the asphalt phase under a mechanical loading of 25 nN. The figure is reproduced from Dourado et al. [52] (under the creative commons attribution license/public domain).

phase), periphase (phase surrounding dispersed phase), and perpetua phase (continuous phase). It is reported that the existence and dominance of these microdomains can be highly influenced by aging, environmental factors, and asphalt modification types.

(iv) Many studies also reported that an asphalt binder consists of network of molecular compounds, observed through electron microscopes. When asphalt is loaded, the fibril network provides the resistance force and contribute to prevent deformation and act as a stitching between the microcracks. The average diameter of molecule fibril of a typical asphalt molecule is 10 micrometers. However, the size of the fibrils can vary due to aging and modification types.

(v) Adhesibility is a very important performance property of asphalt binder that is highly varied depending source, and chemical compositions and types. The adhesive property of asphalt microdomains can be

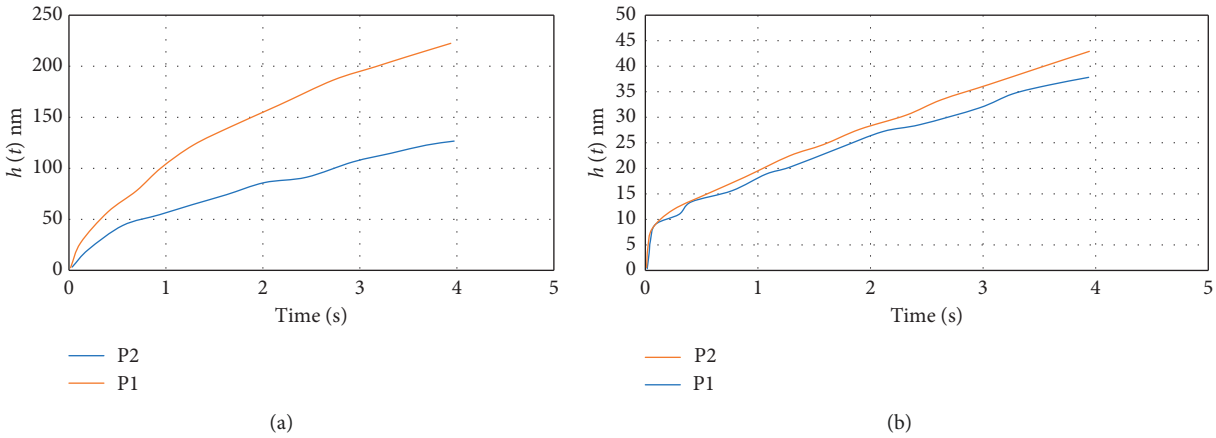

Figure 26: Deformation over time of perpetua (P1) and peri (P2) phases under a creep load of 5 nanonewtons for unaged (a) and aged (b) asphalt samples. The figure is reproduced from Allen [33] (under the creative commons attribution license/public domain).

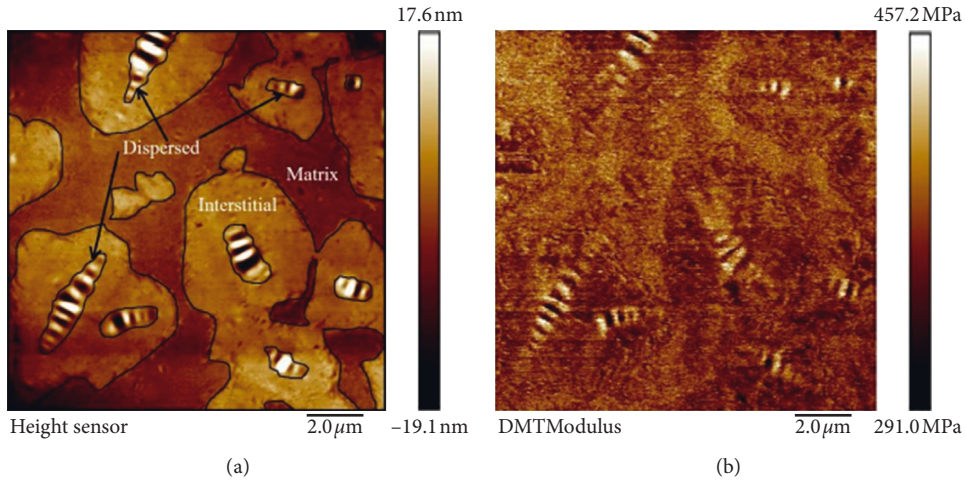

Figure 27: (a) Micrographs of asphalt phases before application of strain and (b) after straining.

estimated using the atomic force technique, and studies reported that the property is significantly varied among the microdomains and the catana phase has the weakest adhesive force component.

(vi) From stiffness perspective, the catana phase is stiffer than perpetua phase, while the perpetua phase was found more viscous than periphase. However, under creep loading, a higher deformation was found in the perpetua phase compared to the catana phase.

Conflicts of Interest

The authors declare that they have no conflicts of interest.

Acknowledgments

The authors would like to acknowledge the contribution of their graduate students in preparation of this manuscript for capturing some of the images in the laboratory or creating the charts after collecting data from the existing literature. They include Mr. M. M. Tariq Morshed, Mr. Feroze Rashid, Mr. Shahriar Alam, Mr. Sumon Roy from Arkansas State University in USA, and Farhana Akter from Memorial University in Canada. Also, the authors would like to acknowledge all the researchers and their great works that generated a great amount of data to understand asphalt binder at molecular level.

References

[1] UPM, *Unique Paving Materials Corp*, 2018, https://www.uniquepavingmaterials.com/asphalt-paving-throughout-history/.

[2] E. R. Brown, P. S. Kandhal, F. L. Roberts et al., *Hot Mix Asphalt Materials, Mixture Design and Construction*, Worldcat, National Asphalt Pavement Association Research and Education Foundation, Lanham, MD, USA, 2nd edition, 1996.

[3] P. W. Jennings, J. A. Pribanic, M. A. Desando et al., *Binder Characterization and Evaluation by Nuclear Magnetic Resonance Spectroscopy*, National Research Council, Washington, DC, USA, 1993.

[4] P. Jennings, M. Desando, M. Raub, R. Moats, T. Mendez, and F. F. Stewart, "NMR spectroscopy in the characterization of

eight selected asphalts," *Fuel Science and Technology International*, vol. 10, pp. 887–907, 1992.

[5] K. Stangl, A. Jäger, and R. Lackner, "Microstructure-based identification of bitumen performance," *Road Materials and Pavement Design*, vol. 7, pp. 111–142, 2006.

[6] P. K. Das, H. Baaj, S. Tighe, and N. Kringos, "Atomic force microscopy to investigate asphalt binders: a state-of-the-art review," *Road Materials and Pavement Design*, vol. 17, no. 3, pp. 693–718, 2016.

[7] Y. Veytskin, C. Bobko, and C. Castorena, "Nanoindentation and atomic force microscopy investigations of asphalt binder and mastic," *Journal of Materials in Civil Engineering*, vol. 28, no. 6, article 04016019, 2016.

[8] M. Guo, Y. Tan, J. Yu, Y. Hou, and L. Wang, "A direct characterization of interfacial interaction between asphalt binder and mineral fillers by atomic force microscopy," *Materials and Structures*, vol. 50, no. 2, pp. 1–12, 2017.

[9] L. D. Poulikakos and M. N. Partl, "Investigation of porous asphalt microstructure using optical and electron microscopy," *Journal of Microscopy*, vol. 240, no. 2, pp. 145–154, 2010.

[10] D. Lesueur, "The colloidal structure of bitumen: consequences on the rheology and on the mechanisms of bitumen modification," *Advances in Colloid and Interface Science*, vol. 145, no. 1-2, pp. 42–82, 2009.

[11] L. Champion, J. F. Gerard, J. P. Planche, D. Martin, and D. Anderson, "Low temperature fracture properties of polymer-modified asphalts relationships with the morphology," *Journal of Materials Science*, vol. 36, no. 2, pp. 451–460, 2001.

[12] K. Dunn, G. V. Chilingarian, H. Lian, Y. Y. Wang, and T. F. Yen, "Chapter 11 analysis of asphalt and its components by thin-layer chromatography," in *Developments in Petroleum Science*, Elsevier, Amsterdam, Netherlands, 2000.

[13] O. C. Mullins, A. E. Pomerantz, A. B. Andrews, and J. Y. Zuo, "Asphaltenes explained for the nonchemist," *Petrophysics*, vol. 56, no. 3, pp. 266–275, 2015.

[14] L. Eberhardsteiner, F. Josef, B. Hofko et al., "8th international RILEM symposium on testing and characterization of sustainable and innovative bituminous materials, SIB 2015," *International Journal of Pavement Research and Technology*, vol. 7, no. 1, pp. 411–421, 2014.

[15] R. L. Griffin, W. C. Simpson, and T. K. Miles, "Influence of composition of paving asphalt on viscosity, viscosity-temperature susceptibility, and durability," *Journal of Chemical & Engineering Data*, vol. 4, no. 4, pp. 349–354, 1959.

[16] B. Hofko, L. Eberhardsteiner, J. Füssl et al., "Impact of maltene and asphaltene fraction on mechanical behavior and microstructure of bitumen," *Materials and Structures*, vol. 49, no. 3, pp. 829–841, 2016.

[17] Z. Kraus, *The Morphology of Polymer Modified Asphat and Its Relationsh to Rhelogy and Durability*, Texas A&M University, College Station, TX, USA, 2008.

[18] L. Loeber, O. Sutton, and J. Morel, "New direct observations of asphalts and asphalt binders by scanning electron microscopy and atomic force microscopy," *Journal of Microscopy*, vol. 182, pp. 32–39, 1996.

[19] R. Jahangir, D. Little, and A. Bhasin, "Evolution of asphalt binder microstructure due to tensile loading determined using AFM and image analysis techniques," *International Journal of Pavement Engineering*, vol. 16, no. 4, pp. 337–349, 2014.

[20] A. T. Pauli, R. W. Grimes, A. G. Beemer, T. F. Turner, and J. F. Branthaver, "Morphology of asphalts, asphalt fractions and model wax-doped asphalts studied by atomic force microscopy," *International Journal of Pavement Engineering*, vol. 12, no. 4, pp. 291–309, 2011.

[21] H. R. Fischer, E. C. Dillingh, and C. G. M. Hermse, "On the microstructure of bituminous binders," *Road Materials and Pavement Design*, vol. 15, no. 1, pp. 1–15, 2014.

[22] L. M. Rebelo, P. N. Cavalcante, J. S. De Sousa, J. M. Filho, S. A. Soares, and J. B. Soares, "Micromorphology and microrheology of modified bitumen by atomic force microscopy micromorphology and microrheology of modified bitumen by atomic force microscopy," *Road Materials and Pavement Design*, vol. 15, no. 2, pp. 300–311, 2014.

[23] A. T. Pauli, *Chemomechanics of Damage Accumulation and Damage-Recovery Healing in Bituminous Asphalt Binders*, Delft University of Technlogy, Delft, Netherlands, 2014.

[24] J. F. Masson, V. Leblond, and J. Margeson, "Bitumen morphologies by phase-detection atomic force microscopy," *Journal of Microscopy*, vol. 221, no. 1, pp. 17–29, 2006.

[25] H. Soenen, X. Lu, and P. Redelius, "The morphology of bitumen-SBS blends by UV microscopy," *Road Materials and Pavement Design*, vol. 9, no. 1, pp. 97–110, 2008.

[26] H. Soenen, J. Besamusca, H. R. Fischer et al., "Laboratory investigation of bitumen based on round robin DSC and AFM tests," *Materials and Structures*, vol. 47, no. 7, pp. 1205–1220, 2013.

[27] I. Menapace, E. Masad, and A. Bhasin, "Effect of treatment temperature on the microstructure of asphalt binders: insights on the development of dispersed domains," *Journal of Microscopy*, vol. 262, no. 1, pp. 12–27, 2016.

[28] R. G. Allen, D. N. Little, A. Bhasin, and C. J. Glover, "The effects of chemical composition on asphalt microstructure and their association to pavement performance," *International Journal of Pavement Engineering*, vol. 15, no. 1, pp. 9–22, 2014.

[29] S. N. Nahar, M. Mohajeri, A. J. M. Schmets, A. Scarpas, M. F. C. van de Ven, and G. Schitter, "First observation of blending-zone morphology at interface of reclaimed asphalt binder and virgin bitumen," *Transportation Research Record: Journal of the Transportation Research Board*, vol. 2370, no. 1, pp. 1–9, 2013.

[30] S. Zhao, S. N. Nahar, A. J. M. Schmets, B. Huang, X. Shu, and T. Scarpas, "Investigation on the microstructure of recycled asphalt shingle binder and its blending with virgin bitumen," *Road Materials and Pavement Design*, vol. 16, no. 1, pp. 21–38, 2015.

[31] S. N. Nahar, *Phase-Separation Characteristics of Bitumen and Their Relation to Damage-Healing*, Delft University of Technology, Delft, Netherlands, 2016.

[32] R. G. Allen, D. N. Little, D. M. Asce, and A. Bhasin, "Structural characterization of micromechanical properties in asphalt using atomic force microscopy," *Journal of Materials in Civil Engineering*, vol. 24, no. 10, pp. 1317–1327, 2012.

[33] R. Allen, *Structural Characterization of Micromechanical Properties in Asphalt Using Atomic Force Microscopy*, Texas A&M University, College Station, TX, USA, 2010.

[34] L. M. Rebelo, J. S. De Sousa, A. S. Abreu et al., "Aging of asphaltic binders investigated with atomic force microscopy," *Fuel*, vol. 117, pp. 15–25, 2014.

[35] Q. Qin, M. J. Farrar, A. T. Pauli, and J. J. A.. Morphology, "Thermal analysis and rheology of sasobit modified warm mix asphalt binders," *Fuel*, vol. 115, pp. 416–425, 2014.

[36] S. Dos Santos, M. N. Partl, and L. D. Poulikakos, "Newly observed effects of water on the microstructures of bitumen

surface," *Construction and Building Materials*, vol. 71, pp. 618–627, 2014.
[37] X. Yu, Y. Wang, and T. Wei, "The viscosity-reducing mechanism of organic wax additive on CRMA," *Journal of Wuhan University of Technology*, vol. 28, no. 4, pp. 726–732, 2013.
[38] M. Nazzal, S. Kaya, and L. Abu-qtaish, *Evaluation of WMA Healing Properties Using Atomic Force Microscopy*, Springer, Berlin, Germany, 2012.
[39] J.-F. Su, J. Qiu, E. Schlangen, and Y.-Y. Wang, "Experimental investigation of self-healing behavior of bitumen/microcapsule composites by a modified beam on elastic foundation method," *Materials and Structures*, vol. 48, no. 12, pp. 4067–4076, 2014.
[40] J. Qiu, *Self Healing of Asphalt Mixtures: Towards a Better Understanding of the Mechanism*, Delft University of Technology, Delft, Netherlands, 2012.
[41] R. Kim, D. Little, and R. Burghardt, "SEM Analysis on Fracture and Healing of Sand-Asphalt Mixture," *Journal of Materials in Civil Engineering*, vol. 3, no. 2, pp. 140–153, 1991.
[42] S. J. Rozeveld, E. Eugene Shin, A. Bhurke, L. France, and L. T. Drzal, "Network morphology of straight and polymer modified asphalt cements," *Microscopy Research and Technique*, vol. 38, no. 5, pp. 529–543, 1997.
[43] Thermofisher. Nanodevices, 2018, https://www.fei.com/materials-science/nanodevices/.
[44] J. Gaskin, *On Bitumen Microstructure and the Effects of Crack Healing*, University of Nottingham, Nottingham, UK, 2013.
[45] E. Shin, A. Bhurke, E. Scott, S. Rozeveld, and L. Drzal, "Microstructure, morphology, and failure modes of polymer-modified asphalts," *Transportation Research Record: Journal of the Transportation Research Board*, vol. 1535, pp. 61–73, 1996.
[46] M. J. Khattak, A. Khattab, P. Zhang, H. R. Rizvi, and T. Pesacreta, "Microstructure and fracture morphology of carbon nano-fiber modified asphalt and hot mix asphalt mixtures," *Materials and Structures*, vol. 46, no. 12, pp. 2045–2057, 2013.
[47] K. Nikooyeh, *Phase Behavior of Asphaltenes in Organic Media*, University of Alberta, Edmonton, AB, Canada, 2012.
[48] M. Jasso, *The Mechanism of Modification and Properties of Polymer Modified Asphalts*, University of Calgary, Calgary, AB, Canada, 2016.
[49] H. Fischer, H. Stadler, and N. Erina, "Quantitative temperature-depending mapping of mechanical properties of bitumen at the nanoscale using the AFM operated with PeakForce TappingTM mode," *Journal of Microscopy*, vol. 250, no. 3, pp. 210–217, 2013.
[50] Z. Hossain, F. Rashid, I. Mahmud, and M. Rahaman, "Morphological and nanomechanical characterization of industrial and agricultural waste–modified asphalt binders," *International Journal of Geomechanics*, vol. 17, no. 3, article 04016084, 2016.
[51] X. Yu, N. A. Burnham, R. B. Mallick, and M. Tao, "A systematic AFM-based method to measure adhesion differences between micron-sized domains in asphalt binders," *Fuel*, vol. 113, pp. 443–447, 2013.
[52] E. R. Dourado, R. A. Simao, and L. F. M. Leite, "Mechanical properties of asphalt binders evaluated by atomic force microscopy," *Journal of Microscopy*, vol. 245, no. 2, pp. 119–128, 2012.
[53] T. Pauli, W. Grimes, A. Cookman, S. Huang, and M. Asce, "Adherence Energy of Asphalt Thin Films Measured by Force-Displacement Atomic Force Microscopy," *Journal of Materials in Civil Engineering*, vol. 26, no. 12, pp. 1–11, 2014.
[54] A. S. Al-rawashdeh and S. Sargand, "Performance assessment of a warm asphalt binder in the presence of water by using surface free energy concepts and nanoscale techniques," *Journal of Materials in Civil Engineering*, vol. 26, no. 5, pp. 803–811, 2014.
[55] Å. L. Lyne, V. Wallqvist, and B. Birgisson, "Adhesive surface characteristics of bitumen binders investigated by atomic force microscopy," *Fuel*, vol. 113, pp. 248–256, 2013.
[56] R. A. Tarefder and A. Zaman, "Characterization of asphalt materials for moisture damage using atomic force microscopy and nanoindentation," in *Nanotechnology in Civil Infrastructure*, pp. 237–256, Springer, Berlin, Germany, 2011.
[57] R. A. Tarefder and S. Ahsan, "Neural network modelling of asphalt adhesion determined by AFM," *Journal of Microscopy*, vol. 254, no. 1, pp. 31–41, 2014.
[58] R. G. Allen, D. N. Little, A. Bhasin, and R. L. Lytton, "Identification of the composite relaxation modulus of asphalt binder using AFM nanoindentation," *Journal of Materials in Civil Engineering*, vol. 25, no. 4, pp. 530–539, 2012.
[59] L. A. Qtaish, *The Use of Atomic Force Microscopy in Evaluating Warm Mix Asphalt*, Ohio University, Athens, OH, USA, 2013.